Calculating Ground-State-Energy of $LiCoO_2$ by using Fragment molecular orbital-based Variational Quantum Eigensolver

Yoonho Choi[1] and Doha Kim[1], Doyeon Kim[1]

Younghun Kwon

[1] Department of Applied Physics, Hanyang University, Ansan, 15588, Republic of Korea
cyh195535@hanyang.ac.kr

Abstract. The Variational Quantum Eigensolver (VQE) is a quantum computing algorithm designed to calculate the ground-state energy. VQE has been highly anticipated for its potential effectiveness in fields such as new material development, drug discovery, and battery technology. However, current quantum computers are limited by the number of available qubits, which poses challenges for applying VQE to large and complex molecules in industrial applications. To address this issue, we propose using the FMO-VQE approach to tackle a real-world problem. The Fragment Molecular Orbital (FMO) method divides a system into smaller fragments for processing. While Ref [1] discusses the FMO method within the VQE framework, it only considers hydrogen clusters. Therefore, the effectiveness of the FMO-VQE approach seems to be limited to very simple cases. In this study, we aim to evaluate the effectiveness of the FMO-VQE approach in a real-world problem. Specifically, we consider a more complex material composed of different atoms, such as $LiCoO_2$, which is used as a cathode material for lithium-ion batteries. We evaluate the ground-state energy of $LiCoO_2$ using the FMO-VQE method, demonstrating its utility. By employing this approach, the number of required qubits is reduced from 24 to a maximum of 14, while maintaining accuracy comparable to classical methods. This study shows that the proposed FMO-VQE algorithm can mitigate size-related constraints, enabling the VQE algorithm to be applied to larger molecular systems. This advance paves the way for the successful implementation of the VQE algorithm in fields such as battery technology and drug discovery.

Keywords: VQE, Quantum Computing, Lithium-ion batteries

1 Introduction

The ground state and energy of a molecule are crucial for understanding the bonds between molecules and their structural properties. This information is essential in various areas of chemical research, including the development of new drugs and the creation of advanced anode materials for secondary batteries.

Currently, the ground state energy of a molecule is typically calculated using classical computers. However, as the number of atoms in a molecule increases or the atomic number of the elements involved becomes larger, the number of particles and their interactions also grows exponentially. These interactions are represented in the molecule's Hamiltonian, which requires substantial computational resources and memory to process. As a result, calculating the ground state energy of large molecules using classical computers becomes increasingly difficult.

Quantum computers are an emerging field of technology. Unlike classical computers, quantum computers use qubits. A qubit, known as a quantum bit, is a superposition of 0 and 1 states, whereas a bit in classical computers represents only 0 or 1. This gives quantum computers the potential to calculate the ground state energy of a molecule. In other words, the characteristics of quantum computers imply that when a classical computer would require an exponential increase in memory, a quantum computer can achieve the same with only a polynomial increase in qubits. Therefore, even large molecules that are currently infeasible to compute on classical computers can be processed by quantum computers.

The Quantum Phase Estimation (QPE) algorithm is used to calculate the eigenvalues and eigenstates of a unitary matrix on a quantum computer, and it can be applied to determine the ground state energy of a molecule. However, QPE is known for its high accuracy but also requires a large number of qubits to implement. Currently, quantum computers are considered to be at the level of noisy intermediate-scale quantum devices (NISQs). NISQ refers to quantum computers that are noisy and have an intermediate number of qubits. While current quantum computers are still noisy, lack precision, and have relatively few qubits—typically in the tens or hundreds—this makes it difficult to implement QPE effectively.

The Variational Quantum Eigensolver (VQE) is an algorithm designed to solve eigenvalue problems using NISQ-level quantum computers, utilizing both quantum and classical computing. VQE applies variational principles to construct a parameterized trial wavefunction, which is then used to determine the basis of the molecular Hamiltonian. The algorithm iterates by adjusting the parameters until the basis value converges to a constant, providing an upper bound for the ground state energy of the molecule. In this process, the molecular Hamiltonian and the trial wavefunction are represented by quantum circuits, with the expectation value computation performed by the quantum computer. The optimization of the trial wavefunction's parameters, however, is carried out by a classical computer. Unlike QPE, VQE does not require many qubits, and since the optimization, which is challenging for current quantum computers, is handled by a classical computer, there is considerable optimism about the potential for quantum computers to be commercialized in the NISQ era.

However, current quantum computers are still plagued by errors, and their accuracy significantly decreases as the circuit depth increases. Furthermore, the number of qubits available is limited, which is insufficient for calculating the ground state energy of very large molecules.

To address these challenges, one promising approach is the Fragment Molecular Orbital method-based Variational Quantum Eigensolver (FMO-VQE). FMO-VQE was first proposed by Lim et al. (ref 1) as an algorithm that applies the FMO method. The FMO method, a classical technique, approximates the ground-state energy of a molecule by dividing it into smaller fragments, then calculating the ground-state energy for individual monomers and dimers. These results are then used to estimate the total ground-state energy of the entire molecule. By breaking the molecule into smaller pieces, the size of the system that needs to be considered in the overall calculation is reduced, which in turn lowers the number of qubits required and the depth of the quantum circuit.

Although Lim et al. proposed the FMO-VQE method, they were only able to assess its effectiveness on hydrogen clusters, not on more complex molecules composed of various atoms.

Therefore, it is natural to question the effectiveness of the FMO-VQE method in real-world applications. In this study, we investigate the performance of FMO-VQE by considering LiCoO2, a representative material used as an anode in secondary batteries. We calculate the ground state energy of LiCoO2 and compare it with classical computer calculations. Additionally, we compare the accuracy of FMO-VQE with classical VQE to evaluate the feasibility of FMO-VQE in the NISQ era.

2   Method

2.1   Lithium-ion battery

  Lithium-ion batteries are widely used secondary batteries in various industries. A lithium-ion battery consists of an anode material, a cathode material, and an electrolyte, with lithium oxide typically used as the anode material. This compound has a layered structure of CoO_2^- oxide, with Li^+ ions bonded between each layer. The energy charge of the battery depends on the extent to which the lithium ions are oxidized in the oxide.

Lithium is known to have limited reserves in the world, prompting the need for sustainable solutions. One such solution is to maximize the energy charged per lithium ion. This is critical both in terms of conserving lithium resources and for advancing battery miniaturization. To calculate the amount of energy stored per lithium ion, it is essential to compute the ground state of the molecule. However, this calculation is typically done using classical methods, and the ability to calculate larger molecules or more complex combinations is limited.

In this study, we demonstrate the application of the VQE algorithm to LiCoO₂ molecules and highlight the potential of quantum computers in the field of battery development.
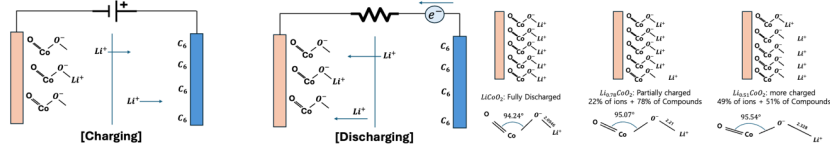

Fig. 1. Left) Schematic of battery charging and discharging, Right) Geometry of compounds by oxidation state

When a voltage is applied to the anode and cathode to supply electrons (i.e., during charging), the Li^+ ions migrate to the cathode. Upon discharging from this charged state, the Li^+ ions from the negative electrode recombine with the positive electrode, as shown in the figure below, and current flows through the resistor. During this process, depending on the oxidation state of lithium, the average geometry of the molecular structure changes, as illustrated in Fig. 1. Therefore, the energy stored in the bulk can be estimated using this geometry. The energy of the molecule is calculated by assuming a gas-phase model, which treats the average oxide structure as a single molecule.

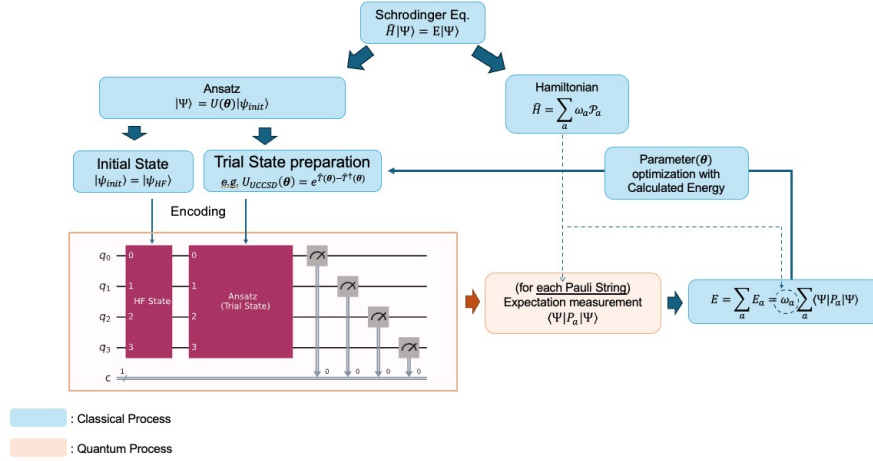## 2.2 VQE(Variational Quantum Eigensolver)

Fig. 2. VQE Pipeline

The Variational Quantum Eigensolver (VQE) algorithm is an eigenvalue problem-solving method first proposed by Peruzzo et al. in [2]. It works by computing the energy in Hilbert space, providing an upper bound on the ground state energy according to the variational principle. VQE calculates the ground state energy of a system by

measuring the energy on a quantum computer and performing optimization on a classical computer. To measure the energy of a system on a quantum computer, the Hamiltonian must be mapped to a form that can be represented as a quantum circuit. Additionally, an arbitrary quantum state needs to be encoded into the circuit for the measurement process.

Hamiltonian

The Hamiltonian of a molecule is represented by the Electronic Structure Hamiltonian as follows:

$$\hat{H}_{el}(r) = -\sum_i \frac{1}{2} \nabla_{r_i}^2 - \sum_I \sum_i \frac{Z_I}{|R_I - r_i|} + \sum_i \sum_{j>i} \frac{1}{|r_i - r_j|} \tag{1}$$

where r_i denotes the position vector of the i-th electron, R_I denotes the position of the I-th nucleon, and Z_I is the atomic number of the I-th nucleon. To map this Hamiltonian to the Pauli gates, we express it in second quantized form using fermionic creation/annihilation operators, as follows:

$$\hat{H}_{el} = \sum_{p,q} h_{pq} \hat{a}_p^\dagger \hat{a}_q + \frac{1}{2} \sum_{p,q,r,s} h_{pqrs} \hat{a}_p^\dagger \hat{a}_q^\dagger \hat{a}_r \hat{a}_s, \tag{2}$$

$$where, \ h_{pq} = \langle \phi_p | \hat{H}_{el} | \phi_q \rangle, \ h_{pqrs} = \langle \phi_p \phi_q | \hat{H}_{el} | \phi_r \phi_s \rangle \tag{3}$$

Fermionic operators can be mapped to Pauli gates using Jordan-Wigner mapping, Parity mapping, and bravyi-kitaev mapping. In this experiment, we will use the Parity mapping method. Parity mapping expresses the creation-annihilation operator through a Pauli gate by corresponding the parity of the ith qubit to the parity of the electron occupancy of the ith orbital. In this case, the parity of the α-spin and β-spin of the molecule can be utilized to reduce the number of qubits required by two. The resulting Hamiltonian of the mapping is represented by a Pauli string ($\mathcal{P}_a$) and its weights or linear coefficients (ω_a) as shown below.

$$\hat{H} = \sum_a \omega_a \mathcal{P}_a \tag{4}$$

Ansatz

To represent arbitrary quantum states, we construct a parameterized quantum circuit (PQC) with linear coefficients corresponding to each basis as parameters. The performance of the ansatz is difficult to evaluate, and it is not known a priori which ansatz is better for different systems. Therefore, in this experiment, we use two different ansatzes to achieve better results.

Two-Local (Efficient SU2) Ansatz

The quantum state of a single qubit is represented by a rotation gate with two arbitrary angles on the Bloch sphere. If the angle of the rotation gate is treated as a parameter,

and the entanglement — a property of qubits in a multi-qubit system — is expressed using a CNOT gate, then the quantum state of an arbitrary multi-qubit system can be expressed using these parameters.
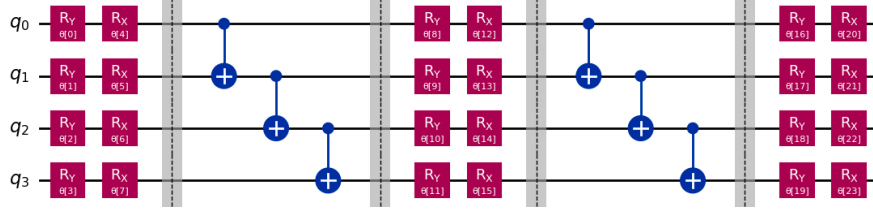

Fig. 3. Two_Local Ansatz Example on a 4-Qubit System

The construction of the Two-Local Ansatz does not require an interpretation of the Hamiltonian. It is a representation of an arbitrary quantum state that is encoded in hardware, making it hardware-efficient.

UCCSD Ansatz

Through second quantization, we express the Hamiltonian operator in terms of the basis of the molecular orbitals of the system. Ultimately, the state we are looking for is represented in the same Hilbert space as the Hamiltonian. By using the same spin-orbitals as the basis, we can express any quantum state in the Hilbert space where the Hamiltonian exists. In this way, the quantum state is expressed through Coupled-Cluster Theory, using the spin-orbit wavefunction of the molecule as the basis. When considering only second-order excitations, it is represented as a unitary operator, UCCSD (Unitary Coupled-Cluster Singles and Doubles), with the following expression:

$$\hat{T} = \hat{T}_1 + \hat{T}_2, \; (Cluster \; operator) \tag{5}$$

$$where, \; \hat{T}_1 = \sum_{i,a} c_i^a \hat{a}_a^\dagger \hat{a}_i \, , \; \hat{T}_2 = \sum_{ijab} t_{ij}^{ab} \hat{a}_a^\dagger \hat{a}_b^\dagger \hat{a}_j \hat{a}_i$$

$$|\Psi\rangle_{UCCSD} = e^{\hat{T}-\hat{T}^\dagger} |\psi_{ref}\rangle \tag{6}$$

The states are represented by creation and annihilation operators, which can be encoded in quantum circuits using either Jordan-Wigner mapping or parity mapping. The energy of the system is calculated by measuring the expectation value for each Pauli string in the Hamiltonian within these quantum circuits. By iterating over these measurements and optimizing the parameters of the ansatz to minimize the calculated energy, an upper bound on the ground state energy is determined. The resulting minimum corresponds to the ground state energy calculated by the VQE algorithm for the system.
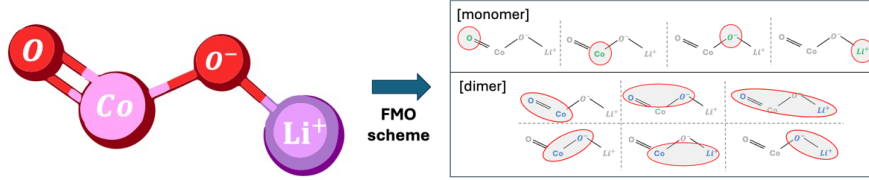
2.3   FMO(Fragmental Molecular orbital)

Fig. 4. An example of the FMO scheme in $LiCoO_2$

The FMO method is a method that divides a whole molecular system into smaller system fragments and approximates the energy of the whole system by using the energy of one fragment (monomer) and the energy of pairs of fragments (dimers). When calculating the ground state energy of a molecule by the usual method, the computational complexity is exponential in the size of the system. However, the FMO method can effectively reduce the computational complexity by dividing a large system into parts. The FMO method has two main steps. The first is the FMO-based restricted Hartree-Fock (FMO-RHF) process, which calculates the RHF through the Hamiltonian of monomers and dimers. The Hamiltonian of monomer($\hat{H}_A$) and the Hamiltonian of dimer($\hat{H}_{AB}$) are as follows.

$$\hat{H}_A = \sum_{i \in A}\left[-\frac{\nabla^2_{r_i}}{m_e} - \sum_I \frac{Z_I}{|r_i - R_I|} + \sum_{C \neq A}^{N_{tot}} \int dr' \frac{\rho_J(r')}{|r_i - r'|}\right] + \sum_{i \in A}\sum_{i < j \in A}\frac{1}{|r_i - r_j|} \qquad (7)$$

$$\hat{H}_{AB} = \sum_{i \in A,B}\left[-\frac{\nabla^2_{r_i}}{m_e} - \sum_I \frac{Z_I}{|r_i - R_I|} + \sum_{C \neq A,B}^{N_{tot}} \int dr' \frac{\rho_J(r')}{|r_i - r'|}\right] + \sum_{i \in A,B}\sum_{i < j \in A,B}\frac{1}{|r_i - r_j|} \qquad (8)$$

(Where A,B are the respective fragments. C refers to the fragments that are not included in monomer A or dimer AB, and the term $\rho_J(r')$ is the electric charge density of the fragments outside the monomer or dimer.) By calculating the RHF of each monomer and dimer through the Hamiltonian above, we can get $E^{FMO-RHF}$, which can be expressed as follows.

$$E^{FMO2-RHF} = E^{FMO1-RHF} + \Delta E^{FMO2-RHF} \qquad (9)$$

$$E^{FMO1-RHF} = \sum_A^N E_A \qquad (10)$$

$$\Delta E^{FMO2-RHF} = \sum_{A>B}^N \left[E_{IJ} - E_I - E_J\right] \qquad (11)$$

In the above equations, N refers to all fragments. From the above equations, we can get the HF energy including the electrostatic potential of the whole molecule. The next step is to proceed with FMO based coupled-cluster (FMO-CC). This process is performed to obtain a more accurate value of the FMO-RHF energy, and since this process does not include the electrostatic potential, the Hamiltonian can be calculated using the Electronic Structure Hamiltonian defined earlier. The process of calculating the total energy (E^{FMO-CC}) and correlation energy ($E^{FMO-corr}$) obtained through FMO-CC is as follows.

$$E^{FMOn-CC} = E^{FMOn-RHF} + E^{FMOn-corr} \tag{12}$$

$$E^{FMO2-corr} = E^{FMO1-corr} + \Delta E^{FMO2-corr} \tag{13}$$

$$E^{FMO1-corr} = \sum_A^N E_I^{corr} \tag{14}$$

$$\Delta E^{FMO2-corr} = \sum_{A>B}^N \left(E_{IJ}^{corr} - E_J^{corr} - E_I^{corr} \right) \tag{15}$$

In the above, the FMO-RHF and FMO-CC processes should be separated because the Hamiltonian used in the two processes may be different, and the FMO-CC process should proceed after the SCF calculation of FMO-RHF converges. However, in this experiment, the electrostatic potential term in the FMO-RHF Hamiltonian was approximated by ignoring it, so each process was carried out consecutively and the total energy was calculated from the obtained monomer and dimer energies as follows.

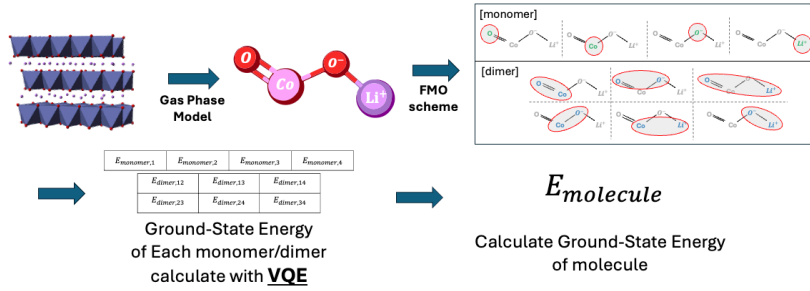## 2.4 FMO-VQE (Fragment molecular orbital-based Varational Quantum Eigensolver)

Fig. 5. An illustration of applying the FMO/VQE method assuming a gas phase model

FMO-VQE is an algorithm first introduced by Lim et al. that combines the VQE algorithm with the FMO method. In the VQE algorithm, the Hemiltonian is represented based on the molecular spinorbitals, so it requires as many qubits as the number of molecular spinorbitals. However, the number of qubits is currently limited, so the number of molecules that can be simulated in the existing VQE algorithm is limited. However, if the FMO Method is applied to the existing VQE algorithm, the number of qubits required for a single calculation can be reduced by parallelizing the calculation and simulating the total system in pieces.

Let's compare the number of qubits required with and without the FMO method. Both calculations use Active Space to reduce the number of qubits required. Given the dynamics of the system, excitations in the core orbital of each atom will have a smaller probability than excitations in the valence orbital. Therefore, we will calculate the core orbital, which is less likely to be involved in bonding, as a separate constant, and assume that the space spanned by the wavefunction of the valence orbital of each atom is a Hilbert space. Under these assumptions, the number of qubits required for a conventional VQE calculation is as follows.

Table 1. Orbital structure of each atom

atom	Number of Valence orbital	Number of Valence electron
Li	2	1
O	6	8
Co	10	7

Table 2. Orbital structure of each Fragment

Configuration	Number of Valence orbital	Number of Valence electron
monomer		
Li	2	1
O	6	4
Co	10	7
Dimer		
Li − O	6	5
Li − Co	12	8
O − O	12	8
Co − O	16	11

Therefore, the number of spin orbitals required for the VQE calculation is 24, considering that oxygen has 2. If we use the parity mapper here, we can reduce the number of qubits needed for the calculation by 2, so 22 qubits are needed to solve this system via conventional VQE.

Let's apply the FMO method, where each atom is a fragment, which means that 4 monomers are created and 6 dimer systems need to be calculated. The number of spin-orbitals required for each calculation is shown below (only one is shown for configurations with the same composition).

Therefore, the maximum number of qubits required in the calculation is 14 (using Parity mapper). By applying the FMO method, we can reduce the number of qubits required for the calculation by 8. Furthermore, the potential of this method is in larger systems. When simulating larger molecules such as Ni, Mn, etc. added to the popular $LiCoO_2$ molecule, conventional VQE requires more qubits than the number of valence orbitals of those atoms. However, in FMO/VQE, the increase in the size of the system leads to an increase in the number of fragments, so it is possible to calculate the energy of larger molecules using the same number of qubits.

3 Result

3.1 Monomer/Dimer Energy

Table 3. Energy of Monomer for each Ansatz/Optimizer

UCCSD	Two-Local

System	COBYLA	SPSA	COBYLA	SPSA	COBYLA	SPSA
"Li"	-7.315526	-7.315526	-7.315526	-7.315526	-7.315430	-7.315526
"O"	-73.804150	-73.804150	-73.804150	-73.804150	-73.803074	-73.804150
"Co"	-1365.943920	-1366.002044	-1366.118261	-1366.006785	-1365.740246	-1366.092075

Table 4. Energy of Dimer for each Ansatz/Optimizer for each Oxidation State of Li_xCoO2

[x=1]	UCCSD				Two-Local	
Configuration	COBYLA	SPSA	COBYLA	SPSA	COBYLA	SPSA
"Li-O¹"	-81.036530	-81.062982	_-81.069739_	-81.023626	-80.978418	-81.069703
"Li-O²"	-81.117531	-81.117951	_-81.117956_	-81.094238	-81.030553	-81.117577
"Li-Co"	-1373.429758	-1373.567946	_-1373.618739_	-1373.576316	-1373.512522	-1373.609970
"O-O"	-147.432250	-147.485749	-147.599156	-147.528891	-147.334234	_-147.605860_
"Co-O¹"	-1439.355819	-1439.796790	_-1439.957262_	-1439.315189	-1439.321781	-1439.695408
"Co-O²"	-1439.459214	-1439.788926	-1439.888880	-1439.396154	-1439.727786	_-1439.918488_

[x=0.94]	UCCSD				Two-Local	
Configuration	COBYLA	SPSA	COBYLA	SPSA	COBYLA	SPSA
"Li-O¹"	-81.079066	-81.071382	_-81.084085_	-81.014315	-81.042272	-81.084060
"Li-O²"	-81.119992	-81.119699	_-81.120071_	-81.117758	-81.066772	_-81.120071_
"Li-Co"	-1373.434678	-1373.568648	-1373.569509	-1373.347301	-1373.529010	_-1373.584236_
"O-O"	-147.391974	-147.374393	_-147.608042_	-147.551759	-147.523597	-147.489992
"Co-O¹"	-1439.423661	-1439.843317	_-1439.952027_	-1439.169880	-1439.485884	-1439.803393
"Co-O²"	-1439.393635	-1439.485720	-1439.898848	-1439.210821	-1439.564247	_-1439.986058_

[x=0.78]	UCCSD				Two-Local	
Configuration	COBYLA	SPSA	COBYLA	SPSA	COBYLA	SPSA
"Li-O¹"	-81.074588	-81.076294	_-81.086310_	-81.070688	-81.021452	-81.086299
"Li-O²"	-81.118325	-81.119637	_-81.120088_	-81.097025	-81.058402	-81.119684
"Li-Co"	-1373.206240	-1373.319480	-1373.354329	-1373.591995	-1373.380891	_-1373.725492_
"O-O"	-147.412124	-147.551726	_-147.607067_	-147.517407	-147.166796	-147.560823
"Co-O¹"	-1439.226044	-1439.778362	_-1439.840047_	-1439.319849	-1439.523202	-1439.714842
"Co-O²"	-1439.547179	-1439.828032	_-1439.944688_	-1439.300309	-1439.408856	-1439.738547

[x=0.75]	UCCSD				Two-Local	
Configuration	COBYLA	SPSA	COBYLA	SPSA	COBYLA	SPSA
"Li-O¹"	-81.065682	-81.081421	_-81.086310_	-81.003117	-81.023070	-81.012210
"Li-O²"	-81.119826	-81.120074	_-81.120088_	-81.095257	-81.071903	_-81.120088_
"Li-Co"	-1373.223660	-1373.354256	-1373.328463	-1373.589681	-1373.585003	_-1373.790507_
"O-O"	-147.413053	-147.281268	_-147.607526_	-147.445853	-147.442307	-147.462992
"Co-O¹"	-1439.226044	-1439.778362	_-1439.840047_	-1439.319849	-1439.523202	-1439.714842
"Co-O²"	-1439.388348	-1439.758178	_-1439.857075_	-1439.354511	-1439.479002	-1439.722998

[x=0.66]	UCCSD				Two-Local	
Configuration	COBYLA	SPSA	COBYLA	SPSA	COBYLA	SPSA
"Li-O¹"	-81.053296	-80.984815	_-81.084085_	-81.014315	-81.042272	-81.084060
"Li-O²"	-81.119992	-81.119699	_-81.120071_	-81.117758	-81.066772	_-81.120071_
"Li-Co"	-1373.434678	-1373.568648	-1373.569509	-1373.347301	-1373.529010	_-1373.584236_
"O-O"	-147.391974	-147.374393	_-147.608042_	-147.551759	-147.523597	-147.489992
"Co-O¹"	-1439.423661	-1439.843317	_-1439.952027_	-1439.169880	-1439.485884	-1439.803393
"Co-O²"	-1439.393635	-1439.485720	-1439.898848	-1439.210821	-1439.564247	_-1439.986058_

*All values in the table are in Ha units. The underlined values represent the lowest energy convergence values for each configuration. The configurations with superscripts refer to different dimers with the same composition but different geometric structures.

Li-O[1]: A dimer consisting of O and Li atoms that form a bond.

Li-O[2]: A dimer consisting of O and Li atoms that do not form a bond.

Co-O[1]: A dimer consisting of Co and O atoms forming a single bond.

Co-O[2]: A dimer consisting of Co and O atoms forming a double bond.

Tables 1 and 2 present the VQE calculation results for each monomer and dimer of the LiCoO₂ molecule, divided into fragments. A total of six cases were computed, combining two types of Ansatz and three types of optimizers. Under the conditions of this experiment, the energy of the monomer does not depend on the relative coordinates of each fragment and is therefore independent of the molecular geometry. In other words, even if the oxidation state changes, the calculation results remain the same, meaning the calculation only needs to be performed once.

Regarding optimizer selection, the difference between L-BFGS-B and other optimizers is approximately on the order of 0.1 Ha. This represents a significant error compared to the desired precision. While COBYLA and SPSA are much faster in terms of computation time, L-BFGS-B demonstrates better results when precision is prioritized.

Several configurations are noteworthy when selecting an Ansatz. For the Co-O1 and Li-O1 configurations, the UCCSD Ansatz consistently produced the lowest energy values across all calculations. In contrast, for the Li-Co configuration, the Two_Local Ansatz showed better convergence values than UCCSD for oxidation states other than x=1. However, for configurations such as Co-O2, Li-O, and O-O, the optimal Ansatz varied despite identical fragment structures in each oxidation state. For instance, in the results for Co-O2, the lowest energies were achieved with UCCSD at x=0.78 and x=0.75, while Two_Local outperformed UCCSD at x=1.00, x=0.94, and x=0.66. This suggests that even for systems with similar characteristics, the choice of Ansatz that best represents the system can vary depending on the specific configuration.

The choice of Ansatz ultimately determines how the Hilbert space is represented in each basis. When the space represented by spin orbitals is not large, the difference between different Ansatz selections is minimal. However, as the dimension of the Hilbert space increases, the expressive power of different Ansatz types can diverge significantly.

For systems such as Li-O[1] and Li-O[2] which are represented using approximately 8 spin-orbital wavefunctions as the basis, the energy difference between Ansatz is typically on the order of $10^{-3} Ha$, which is relatively small. However, as the system size grows, the difference becomes more pronounced. For example, in systems like Li-Co

and O-O^2 represented by 12 spin-orbital wavefunctions, or Co-O^1 and Co-O^2 represented by 16 spin-orbital wavefunctions, the difference increases to the order of 10^{-1} Ha. Such differences can significantly impact the precision of the calculated values.

Therefore, the choice of Ansatz can have a substantial impact depending on the system, especially for experiments requiring high precision. It is crucial to evaluate multiple Ansatz and select the optimal one for each specific system to ensure the best possible results.

3.2 Molecular Energy

The $E_{FMO/VQE}$ values in Table 5, 6 represent the ground-state energies of Li_xCoO_2 for each oxidation state(x), calculated using the FMO-VQE methodology proposed in this paper. The E_{FCI} and E_{CCSD} values are obtained using the traditional computational chemistry methods with the GAMESS simulator, corresponding to the Full Configuration Interaction (FCI) and Coupled-Cluster with Single and Double excitations (CCSD) methods, respectively. In the FCI calculations, the Active Core Scheme was used, whereas it was not used in the CCSD calculations. The energy values represent the results obtained from these classical simulation methods, and the error refers to the difference between the FMO-VQE calculation results and those obtained from the traditional methods. Additionally, the accuracy is expressed as the percentage of this error relative to the traditional energy values.

First, let us examine the results of VQE and FCI calculations. FCI is considered the most accurate theoretical calculation method and is often used as a reference value in many chemical calculations. In this experiment, both VQE and FCI used the same Active Core Scheme to approximate the system before calculating the energy, and it was confirmed that the VQE algorithm produced energy values very similar to those obtained from FCI. The smallest error was observed at $x = 0.94$, where the error was -0.005892, resulting in a lower energy value compared to FCI, indicating that the VQE algorithm is highly accurate. On the other hand, at $x = 0.66$ the error was 0.086063, and at $x = 1$ the error was 0.040462, showing a relatively larger difference.

Table 5. Comparison of the energy, error, and accuracy between FMO/VQE and FCI

Oxidation Number (Li_xCoO_2)	$E_{FMO/VQE}$	E_{FCI}	Error	Accuracy(%)
1.00	-1521.203868	-1521.244330	0.040462	99.9973
0.94	-1521.250344	-1521.244451	-0.005892	99.9996
0.78	-1521.239517	-1521.247824	0.008307	99.9995
0.75	-1521.217377	-1521.248807	0.031431	99.9979
0.66	-1521.163133	-1521.249196	0.086063	99.9943

Table 6. Comparison of the energy, error, and accuracy between FMO/VQE and CCSD

Oxidation Number (Li_xCoO_2)	$E_{FMO/VQE}$	E_{CCSD}	Error	Accuracy(%)
1.00	-1521.203868	-1521.342101	0.138232	99.9884
0.94	-1521.250344	-1521.338869	0.088525	99.9919
0.78	-1521.239517	-1521.341358	0.101841	99.9933
0.75	-1521.217377	-1521.340712	0.123336	99.9942
0.66	-1521.163133	-1521.340283	0.177150	99.9909
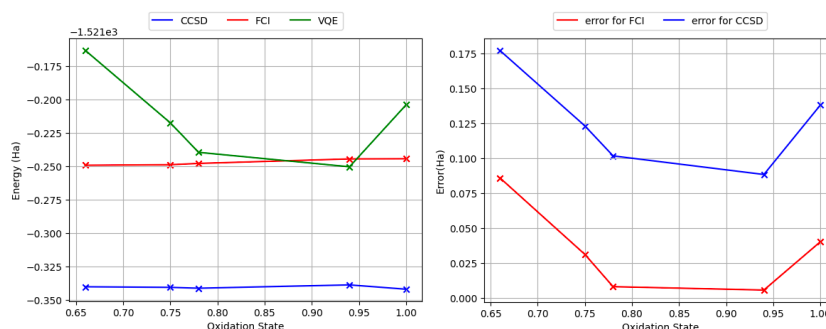
Fig. 6. Energy of FMOVQE, FCI, and CCSD for each oxidation state and the error graph between FMOVQE and FCO, FMOVQE and CCSD

Next, we compare VQE, FCI, and CCSD. FCI is generally regarded as the most precise calculation method and typically provides lower energy convergence values than CCSD. However, in this study, CCSD calculated energy values that were approximately 0.1 Ha lower than FCI for all oxidation states. This difference is attributed to the application of the Active Core Scheme. While FCI employed the Active Core Scheme, CCSD performed calculations on the entire molecule, leading to lower energy values.

By comparing the FMO-VQE algorithm with FCI, we found that the precision of FMO-VQE closely matches that of FCI. This suggests that the FMO-VQE method achieves an accuracy comparable to that of traditional computational methods, demonstrating that quantum computing can deliver practical levels of accuracy. This result implies that, with further advancements in quantum computing technology, it could offer more efficient and accurate calculations than traditional computational chemistry methods. Therefore, this work suggests that the FMO-VQE method provides accuracy nearly identical to classical methods and, with future improvements in quantum computing, could potentially achieve even higher precision. This represents a significant advancement in chemical calculations using quantum computing, showing that it may enable faster and more precise predictions than existing classical methods.

4   Conclusions

As is well known, current quantum computers are limited by the number of available qubits. As a result, applying VQE to large and complex molecules in industrial applications can be challenging. To address this issue, we propose the use of the FMO-VQE approach for real-world problems. Specifically, we evaluated the ground-state energy of LiCoO₂ using the FMO-VQE method. In doing so, we demonstrated that the number of required qubits can be reduced from 24 to a maximum of 14. This shows that the FMO-VQE quantum algorithm can accurately calculate the ground-state energy of the Li_xCoO_2 molecule with high precision, compared to classical simulators, while using a significantly limited number of qubits.

Classical computing methods are not capable of handling the complexity of molecules needed for drug synthesis and the development of new materials. The FMO-VQE algorithm proposed in this study reduces the number of qubits required for these calculations by leveraging the FMO method. Therefore, our results highlight the potential applicability of the FMO-VQE method in future drug synthesis and new material development.

References

1. Hocheol Lim, et al., Fragment molecular orbital-based variational quantum eigensolver for quantum chemistry in the age of quantum computing, Scientific Reports 14, 2422 (2024)
2. Peruzzo A., et al., A variational eigenvalue solver on a photonic quantum processor, Nature Communications 5, 4213 (2014)
3. Jules Tilly, et al. The Variational Quantum Eigensolver: A review of methods and best practices, Physic Reports 986, 1-12 (2022)
4. J.T.Hertz et al. Magnetism and structure of Li_xCoO_2 and comparison to Na_xCoO_2, Department of Chemistry, Princeton University, DOI: 10.1103/PhysRevB.77.075119
5. Kazuo Kitaura, et al., Fragment molecular orbital method: an approximate computational method for large molecules, Chemical Physics Letters 313, 701-706 (1999)
6. Dmitri G. Fedorov, Kazuo Kitaura, Coupled-cluster theory based upon the fragment molecular-orbital method, The Journal of Chemical Physics 123, 134103 (2005)
7. Stewart, Robert F. (1 January 1970). "Small Gaussian Expansions of Slater-Type Orbitals". *The Journal of Chemical Physics*. **52** (1): 431–438. doi:10.1063/1.1672702.